JACS
JOURNAL OF THE AMERICAN CHEMICAL SOCIETY
pubs.acs.org/JACS
Article

Platinum Surface Water Orientation Dictates Hydrogen Evolution Reaction Kinetics in Alkaline Media

Aamir Hassan Shah,[‖] Zisheng Zhang,[‖] Chengzhang Wan, Sibo Wang, Ao Zhang, Laiyuan Wang, Anastassia N. Alexandrova,* Yu Huang,* and Xiangfeng Duan*

Cite This: https://doi.org/10.1021/jacs.3c12934
Read Online
ACCESS | Metrics & More | Article Recommendations | Supporting Information

ABSTRACT: The fundamental understanding of sluggish hydrogen evolution reaction (HER) kinetics on a platinum (Pt) surface in alkaline media is a topic of considerable debate. Herein, we combine cyclic voltammetry (CV) and electrical transport spectroscopy (ETS) approaches to probe the Pt surface at different pH values and develop molecular-level insights into the pH-dependent HER kinetics in alkaline media. The change in HER Tafel slope from ~110 mV/decade in pH 7−10 to ~53 mV/decade in pH 11−13 suggests considerably enhanced kinetics at higher pH. The ETS studies reveal a similar pH-dependent switch in the ETS conductance signal at around pH 10, suggesting a notable change of surface adsorbates. Fixed-potential calculations and chemical bonding analysis suggest that this switch is attributed to a change in interfacial water orientation, shifting from primarily an O-down configuration below pH 10 to a H-down configuration above pH 10. This reorientation weakens the O−H bond in the interfacial water molecules and modifies the reaction pathway, leading to considerably accelerated HER kinetics at higher pH. Our integrated studies provide an unprecedented molecular-level understanding of the nontrivial pH-dependent HER kinetics in alkaline media.

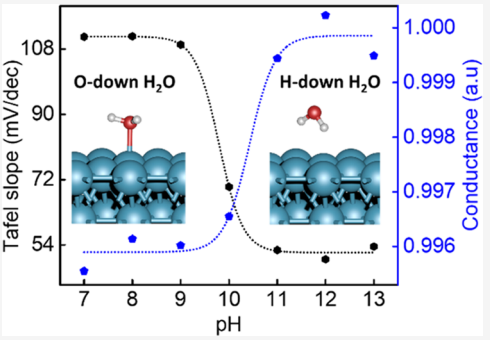

INTRODUCTION

The hydrogen evolution reaction (HER) represents a critical step in water electrolysis, a process used to produce hydrogen gas (H_2) from water. This reaction is fundamental to the production of green hydrogen, which is considered a clean and sustainable energy carrier, especially when coupled with renewable energy sources.[1,2] In general, the HER involves three elementary steps, depending on the electrolyte conditions. The first step is the one-electron reduction of a proton on the Pt electrode to form Pt−H_{ad} (the Volmer step, eqs 1 and 2).

$$H_3O^+ + e^- + Pt \leftrightarrow Pt{-}H_{ad} + H_2O \quad \text{(acidic)} \tag{1}$$

$$H_2O + e^- + Pt \leftrightarrow Pt{-}H_{ad} + OH^- \quad \text{(alkaline)} \tag{2}$$

In the second step, molecular hydrogen (H_2) can be formed either by recombination of two adsorbed hydrogens (Pt−H_{ad}) (Tafel step, eq 3)

$$2Pt{-}H_{ad} \leftrightarrow H_2 + 2Pt \tag{3}$$

or by a simultaneous proton reduction on the electrode surface and its reaction with the surface-bound H (Pt−H_{ad}) to form molecular hydrogen (Heyrovsky step, eqs 4 and 5).

$$Pt{-}H_{ad} + H_3O^+ + e^- \leftrightarrow H_2 + Pt + H_2O \quad \text{(acidic)} \tag{4}$$

$$Pt{-}H_{ad} + H_2O + e^- \leftrightarrow H_2 + Pt + OH^- \quad \text{(alkaline)} \tag{5}$$

The HER kinetics on the platinum (Pt) surface typically displays a distinct dependence on electrolyte pH, with the HER kinetics in alkaline conditions being considerably slower than that in acidic media,[3−5] which has been attributed to a switch of the proton donor from H_3O^+ in acidic conditions to H_2O in alkaline conditions.[6−8] However, the precise switching point and the underlying molecular mechanism have been elusive and a topic of considerable interest. Our recent studies in acidic and neutral electrolytes revealed that the switch of proton source occurred at a pH of around 4 instead of acid/base boundary, which is attributed to a change of Pt surface−H_2O protonation status and associated with Pt surface hydronium pK_a (4.3).[7] However, the change of proton source from H_3O^+ to H_2O cannot explain the HER activity difference in alkaline media.

The hydrogen binding energy (HBE), widely accepted as a thermodynamic descriptor of the HER activity, has been

Received: November 17, 2023
Revised: February 8, 2024
Accepted: February 9, 2024

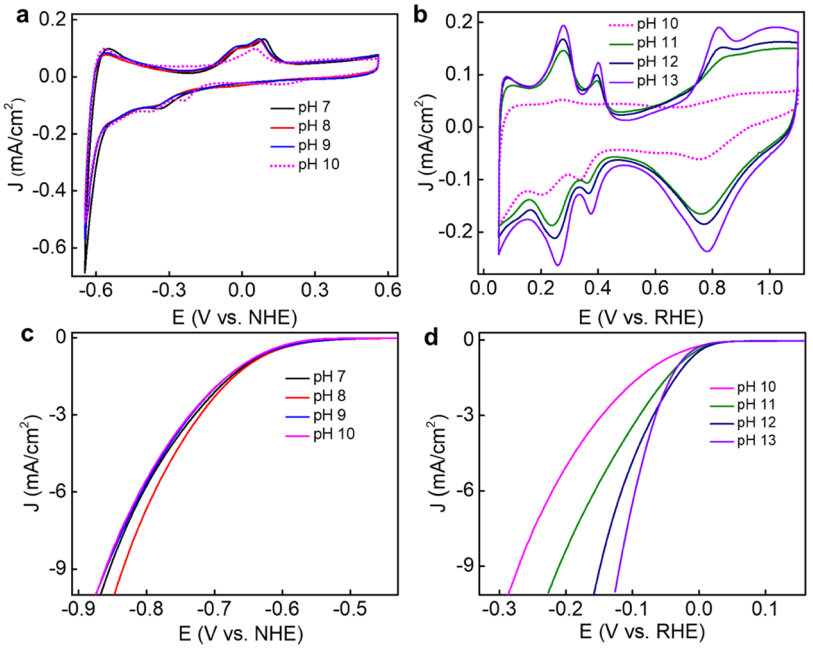

Figure 1. Voltammetric studies in a 0.1 M electrolyte solution with different pH. CV on a stationary Pt disc electrode in a N_2-saturated electrolyte of (a) pH 7, 8, 9, and 10 versus pH-independent NHE scale and (b) pH 10, 11, 12, and 13 versus pH-dependent RHE scale at a scan rate of 100 mV/s (pH was adjusted by KOH and $KClO_4$). IR-corrected HER polarization curves collected in a N_2-saturated electrolyte solution of (c) pH 7, 8, and 9 versus pH-independent NHE scale and (d) pH 10,11,12 and 13 versus pH-dependent RHE scale at a scan rate of 5 mV/s with a rotation rate of 1600 rpm (electrolyte concentration was maintained 0.1 M in all cases, and the pH was adjusted by KOH and $KClO_4$).

frequently used to interpret the pH-dependent HER kinetics.[1,9−14] For example, Sheng et al.[1] and Durst et al.[15] independently suggested that HBE derived from the pH-dependent hydrogen underpotential deposition (H_{upd}) peak may serve as an effective descriptor for interpreting pH-dependent HER kinetics. However, it has been argued by Koper and co-workers that the H_{upd} peak is not only associated with hydrogen adsorption but also convoluted with the hydroxide desorption on step sites.[16] Thus, the pH-dependent H_{upd} peak potential is not an unambiguous indicator of the HBE.

To this end, Koper et al. introduced the potential of zero free charge (pzfc) theory to explain the different HER kinetics in acid and alkaline media.[3] They argued that in acidic media, the pzfc was closer to the HER region, the reorganization energy of interfacial water associated with transporting a proton through an electrical double layer was smaller, and hence the HER kinetics was more facile.[3] However, in alkaline media, the pzfc was far from the HER region (i.e., closer to the OH_{ad} region), leading to a stronger electric field in the HER region and a larger interfacial water reorganization energy and impeding OH^- transfer through the double layer.[3] However, the pzfc theory cannot explain the higher HER kinetics at pH 13 compared to pH 7 as the reorganization energy at pH 13 is expected to be considerably larger than that at pH 7.[17] Besides the aforementioned theories, it has also been suggested that the other factors including water dynamics,[18,19] transport of related intermediates (H_2O^*/OH^*) at the electrode/electrolyte interface,[20,21] and interfacial hydrogen bond networks[22] in alkaline media may also play a critical role in HER kinetics.

Despite extensive aforementioned efforts in comparing the acidic and alkaline media, the HER kinetics within the alkaline (pH > 7) media was often considered pH-independent of the Pt(111) surface[6,23] and much less explored.[17,24−26] Koper ~~and Goyal~~ recently investigated the pH-dependent HER kinetics on ~~a~~ Au electrode in alkaline media and found higher HER activity at higher pH, attributing it to the increased local cation concentration at higher pH that stabilizes the transition state of the rate-determining Volmer step via a favorable interaction with the dissociating water molecule ($*H-OH^{\delta-}-cation^+$).[17] Likewise, Qiao et al. attributed the higher activity in high-pH electrolytes to the locally generated H_3O^+ intermediates, creating a unique acid-like local reaction environment on nanostructured catalytic surfaces and reducing the energy barrier for the overall reaction.[24] Recently, Surendranath et al. also observed a decrease of HER overpotential on Au and Pt electrodes with increasing pH above 10, although the underlying reason was not substantially discussed.[25] Despite these interesting studies and suggestions, a molecular-level understanding of the HER on the Pt electrode in alkaline media has not been developed due to the lack of robust experimental techniques that can reveal molecular-level insights across the Pt−electrolyte interface.

Herein, we address this issue by systematically studying the HER kinetics in nonbuffered alkaline media (pH 7−13) on a polycrystalline Pt electrode surface. Our systematic studies reveal a sharp switch of Tafel slope (from ∼110 mV/decade below pH 10 to ∼53 mV/decade above pH 10) and exchange current density (from ∼0.002 mA/cm^2 below pH 10 to >0.5 mA/cm^2 above pH 10), signifying a switch of the HER kinetics. We further employed electrical transport spectroscopy (ETS) to reveal molecular-level insights into the interfacial water structure on the Pt surface. The ETS conductance signal reveals nearly constant conductance below pH 10 and a notable increase above pH 10, suggesting a change in surface speciation in these two distinct pH regimes. Static and dynamic fixed-potential (FP) density functional theory (DFT) calculations show that the interfacial water molecules adopt the

https://doi.org/10.1021/jacs.3c12934
J. Am. Chem. Soc. XXXX, XXX, XXX−XXX

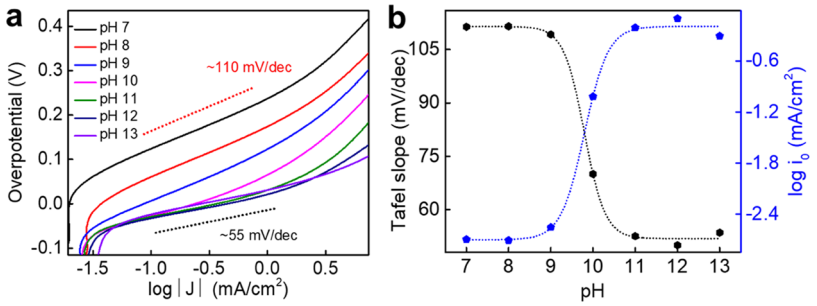

Figure 2. Tafel slope and exchange current density in a 0.1 M electrolyte solution at different pH. (a) Tafel plots in different pH electrolytes collected on a Pt disc electrode with a rotation rate of 1600 rpm at a scan rate of 5 mV/s in a N_2-saturated 0.1 M ionic strength electrolyte solution (pH was adjusted by KOH and $KClO_4$). (b) Plot of Tafel slope values and exchange current density versus electrolyte pH (the dotted lines are guide to the eye).

O-down configuration below pH 11 and flip to the inverse configuration above pH 11, correlating well with the experimentally observed switch of HER kinetics and ETS signals. The switching of the interfacial water molecule orientation to a H-down configuration changes the partial charge distribution and weakens the O−H bond in the interfacial water molecule, which accelerates alkaline Volmer kinetics. This excellent correlation of the experimentally observed switch in Tafel slope, exchange current density, and the ETS conductance signal, with the theory-predicted water orientation change, for the first time, provides a robust molecular-level interpretation of the pH-dependent HER kinetics on the Pt surface in alkaline media. Such molecular-level understanding will be instrumental in guiding further fundamental understanding and eventually the rational design of optimized electrode−electrolyte conditions for alkaline electrolysis.

RESULTS AND DISCUSSION

pH-Dependent Voltammetric Characteristics and HER Activity. The pH dependence of the HER kinetics is an intriguing topic. If we assume protons (hydroniums) as the reactant ($H_3O^+ + e^- + * \rightarrow H_{ad} + H_2O$), the thermodynamic onset potential for HER is expected to be constant on the reversible hydrogen electrode (RHE) scale but negatively shifts 59 mV for each pH increase in the normal hydrogen electrode (NHE) scale ($E_{RHE} = E_{NHE} + 0.059$ pH), according to the Nernst equation ($E = E^0 - 0.059$ pH). On the other hand, the situation could be different in the neutral or alkaline condition, in which the Volmer step ($H_2O + e^- + * \rightarrow H_{ad} + OH^-$) is believed to be rate-limiting. In this case, the onset potential is expected to be independent of the electrolyte pH (thus constant on the NHE scale) because no proton or hydroxide is involved on the reactant side. It has been previously suggested that HER in alkaline media does not involve protons, and one should not expect a pH dependence.[6,23] Thus, a plot on the NHE scale has been frequently used for alkaline media.[6,23] We investigated the voltammetric response of HER on a Pt surface using cyclic voltammetry (CV) in alkaline media of different pH between 7 and 13. Our CV studies reveal that the H_{upd} peak potential from pH 7 to pH 9 is largely independent of pH value, showing a nearly constant peak position or onset potential in the NHE scale (Figure 1a), while the H_{upd} peaks in pH 11−13 show clear pH dependence and thus are compared on the pH-dependent RHE scale (Figure 1b). The CV of pH 10 shows a transition from pH-independent to pH-dependent H_{upd} peaks and hence is presented on both the NHE and RHE scales as a reference point. Overall, the H_{upd} peak intensity increases with an increasing pH and is significantly larger above pH 10. Likewise, the HER polarization curves in pH 7−9 are largely pH-independent (Figure 1c) and show similar HER onset potential on the NHE scale, whereas they show a clear pH dependence in pH 11−13 with a comparable onset potential on the RHE scale but an apparently increased HER activity with increasing pH (Figure 1d). Previous studies of nanostructured Pt[24] or Au[17] electrodes have also shown a similar increase of HER activity with increasing pH in alkaline media.[25,26] We note that there is a study reporting a decrease of HER activity on the Pt(111) electrode with increasing pH from 11 to 13,[3] which is intriguing but not confirmed by other studies yet, to the best of our knowledge.

Considering the potential ambiguity of the NHE to RHE conversion, the Tafel slope and exchange current density give a more reliable evaluation of the reaction kinetics (Figure 2a,b). Importantly, the Tafel slopes and exchange current densities show an apparent transition at pH = 10 (Figure 2b). In particular, the Tafel slopes display a notable switch from a value of ~110 mV/decade below pH 10 to ~53 mV/decade above pH 10 (Figure 2b), suggesting a switch of rate-determining step at around pH 10 and more favorable HER kinetics at higher pH alkaline media. Likewise, the exchange current density versus pH plot also showed two distinct regimes: a much lower value of ~0.002 mA/cm^2 in the electrolyte of pH 7−9, indicating slower kinetics in the neutral pH regime. At pH 10, the intrinsic HER/HOR activity starts to increase with an exchange current density value of ~0.1 mA/cm^2, which reaches beyond ~0.5 mA/cm^2 at pH 11−13. This trend is largely similar to that of the Tafel slope. The slightly lower exchange current density and larger Tafel slope in the case of pH 13 compared to pH 11 and 12 is attributed to the higher local cation concentration at the interface (due to higher pzfc and a larger interfacial electrical field) that negatively impacts the HER/HOR kinetics.[3]

On-Chip In Situ Monitoring of the pH-Dependent Pt Surface Adsorbates. To understand the molecular-level origin of the nontrivial pH dependence of HER kinetics in alkaline media, we employed electrical transport spectroscopic (ETS) studies to directly probe the Pt surface adsorbates at different pH. Using ultrafine Pt nanowires (PtNWs, Figure S1) as a model catalyst,[7,27,28] the ETS approach involves a concurrent measurement of the PtNW conductance during electrochemical studies in a microfabricated on-chip device at different electrochemical potentials (see Figure S2 and ref 27 for the detailed working principle of the technique). In general,

https://doi.org/10.1021/jacs.3c12934
J. Am. Chem. Soc. XXXX, XXX, XXX−XXX

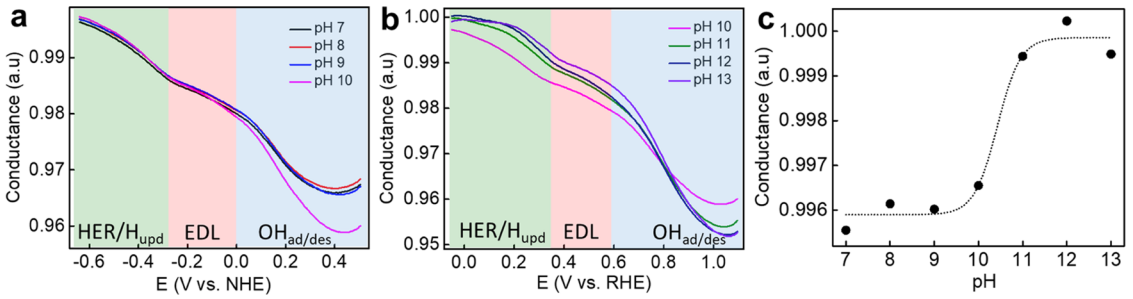

Figure 3. Electrical transport spectroscopy (ETS) measurements. ETS spectra in (a) pH 7−10 versus NHE scale and (b) pH 10−13 versus RHE scale in a 0.1 M electrolyte (ionic strength and pH were maintained by KOH and $KClO_4$). (c) Plot of conductance versus electrolyte pH at −0.59 V versus NHE (from pH 7−10) and 0 V versus RHE (from pH 10−13) (the dotted line is guide to the eye).

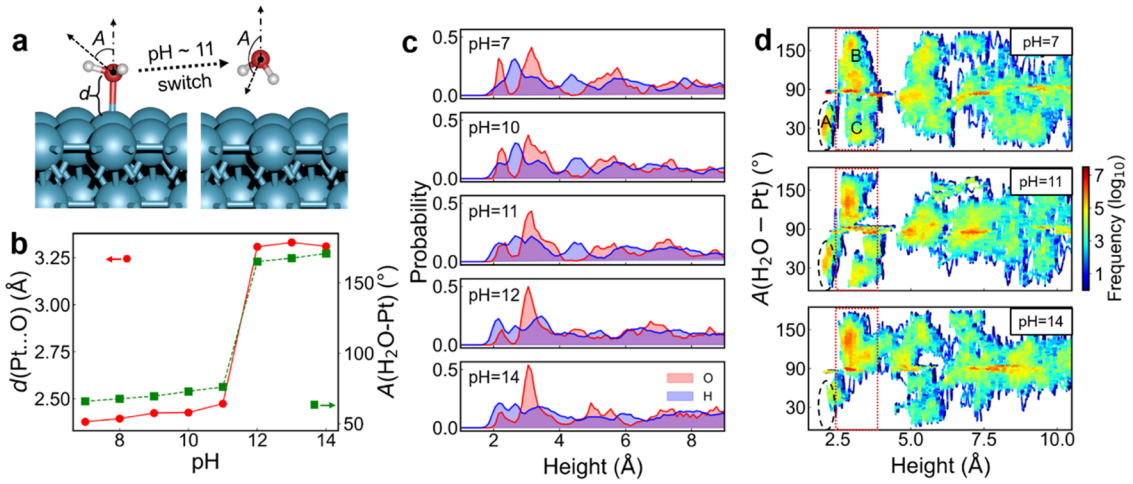

Figure 4. Static and dynamic fixed-potential DFT calculations of the interfacial structure of Pt(111)/water. (a) Structural models of low-pH and high-pH water configurations on Pt(111), with key geometric parameters marked. (b) The Pt−O distance and the water orientation angle in the pH range of 7−14. (c) Spatial probability distribution of O and H in water with respect to the relative height to the Pt surface from fixed-potential ab initio MD simulations at selected pH levels. (d) Statistics of the water orientation angle with respect to the relative height to the Pt surface at selected pH levels. The regions corresponding to adsorbed water (region A) and the contact water layer (region B and C for H-down and O-down waters) are marked by black dashed circles and red dotted boxes, respectively.

the conductance of the ultrafine metallic PtNWs measured in ETS studies is highly sensitive to the exact surface adsorbates due to surface scattering of the conduction electrons but insensitive to the electrostatic or electrochemical potential. The ETS approach thus offers a unique signal transduction pathway to exclusively probe the surface adsorbates with minimum interferences from the electrochemical potentials or the bulk electrolyte environment, which is difficult to achieve with other analytic approaches that are often convoluted with or dictated by the near surface (e.g., electrical double layer) and bulk electrolyte background.

Prior to ETS measurements, the PtNW surface was sufficiently cleaned through repeated cycles in 0.1 M $HClO_4$ between 1.1 and 0.05 V versus RHE in the flow cell until reaching a stable conductance signal (Figure S3). The chamber and device were then thoroughly washed with deionized water to ensure the complete removal of any unintentional surface adsorbents. Finally, the device was used in different pH media to obtain ETS measurements. The ETS studies show that PtNWs generally exhibit a lower conductance in the hydroxide adsorption/desorption potential regime, which is attributed to the more pronounced scattering of the conduction electrons by the strongly bonded OH_{ad}/O_{ad} on the Pt surface in this potential regime.[29] Sweeping the electrochemical potential to the negative direction results in a gradual change of surface adsorbates and thus the corresponding conductance behavior: (i) In the EDL region, the OH_{ad}/O_{ad} molecules are replaced by interfacial H_2O molecules, which reduces the electron scattering and results in an increase in conductance. (ii) By further sweeping the electrode potential to a negative direction, the interfacial H_2O is largely replaced by H_{ad}, which further reduces the scattering and increases the conductance.

The ETS studies in electrolytes with different pH reveal that the conductance is nearly constant in the electrical double-layer (EDL) regime and the HER/H_{upd} potential regime in the electrolyte of pH 7−9, indicating little change in surface speciation on the Pt surface within this pH range (Figure 3a). The shape of the ETS signal at and above pH 10 displays notably different characteristics (Figure 3b). In particular, the conductance showed an increase above pH 10 in the EDL regime and HER/H_{upd} potential regime (Figure 3b). A plot of the conductance in the HER regime versus pH shows a nearly constant conductance from pH 7−9 and a steep rise of the conductance with increasing pH above 10 (Figure 3c). Repeating sets of experiments showed the same trend of pH-dependent conductance change (Figures S4 and S5). Considering that the surface adsorbates in the EDL region are dominated by H_2O_{ad},[30] such an increase of the conductance suggests a change in H_2O_{ad} configuration, likely from a more scattering (lower conductance) O-down

https://doi.org/10.1021/jacs.3c12934
J. Am. Chem. Soc. XXXX, XXX, XXX−XXX

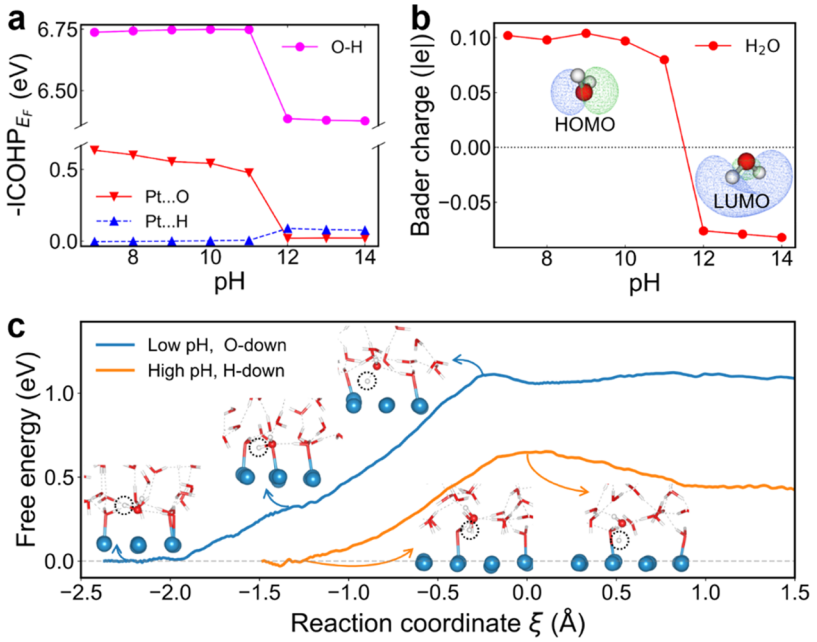

Figure 5. Influence of interfacial water orientation on water dissociation reactivity. (a) The bond strength descriptor, negative integrated crystal orbital Hamilton population (−ICOHP) up to the Fermi level, for Pt−O, Pt−H, and O−H in a pH range of 7−14. (b) Net Bader charge on H_2O at the Pt surface in the pH range of 7−14, with HOMO and LUMO of water shown as insets. (c) The free energy profile of water dissociation for H-down water at high pH and O-down water at low pH. The transferred H is marked by dotted black circles. Notable configurations along the reaction coordinate are shown as insets.

configuration at lower pH to a less scattering (higher conductance) H-down configuration at higher pH. Such a change in water orientation is also in line with previous experimental reports.[31] Interestingly, this switch in the ETS conductance signal at around pH 10 is largely consistent with the evolution of the pH-dependent HER Tafel slopes. The transition point in ETS results indicates that there is an abrupt change in surface speciation at pH 10, which leads to a switch in HER kinetics (Tafel slope) from a Volmer-step-dictated kinetics (with a Tafel slope of ∼110 mV/dec) below pH 10 to a Heyrovsky-step-dictated kinetics (Tafel slope of ∼53 mV/dec) above pH 10.

Theoretical Insight into the Role of pH on Surface Adsorbates. We performed theoretical calculations to further understand the change in surface speciation and explore the molecular-level origin of the switch in the HER kinetics. To probe the nature of the interfacial structural transition that underlies the switching behavior, we used the fixed-potential density functional theory (FP-DFT) technique to locate the most stable adsorption configuration of water on Pt(111) at 0 V_{RHE} in the pH range of 7−14 (Figure S6).[32] Our calculations show that the adsorbed water adopts an O-down configuration below pH 11 but switches to a H-down configuration above pH 11 (Figure 4a). As a result of the configurational change, the Pt−O distance increases from ca. 2.4 to 3.3 Å, and the angle between the H_2O orientation (defined by the vector from O to the midpoint of H's) and the Pt surface normal increases from ca. 60 to 170° (Figure 4b).

To better describe the realistic solvation and dynamics at room temperature,[33] we further performed ab initio molecular dynamics (AIMD) with an explicit water slab of ca. 10 Å thickness and fixed-potential (FP) treatment (Figures S7 and S8) and compared the spatial distribution of O and H atoms (relative to the Pt surface) at selected pH (Figure 4c). As pH increases from 7 to 10, the first O peak at ca. 2.2 Å stays sharp and high, suggesting a large population of directly O-adsorbed water. The H peak at 2.6 Å is significantly higher than the one at 2.1 Å, suggesting the O-down orientation in the contact layer to be dominant. As the pH increases from 10 to 11, the intensity of the first O peak is significantly reduced, suggesting a weakening of the water adsorption via Pt···O. Moreover, the intensity of the H peak at ca. 2.1 Å (corresponding to H-down water) builds up to a comparable level to that of the O-down at pH 11 and becomes dominant beyond pH 12, suggesting a flip of the majority of water molecules in the contact layer. Such a flip is better visualized by the distribution map of water orientation angles (Figure 4d): the adsorbed O-down water (marked by region A) is depleted as the pH increases, and the majority of the interfacial waters shift from an O-down orientation (Region B) to a H-down orientation (Region C). The flipping from the O-down configuration to the H-down configuration upon increasing pH is consistent with a shift from a low conductance state at lower pH to a higher conductance state at higher pH observed in the ETS studies, in which the O-down configuration shows stronger electron scattering and thus lower conductance than the H-down configuration.

The sharp crossover behavior at ∼pH 11 (Figure 4) closely resembles the experimental pH dependence of the HER Tafel slope and exchange density (Figure 2b), which inspires us to quantify the influence of water configurational change on the HER activity. To this end, we performed crystal orbital Hamilton population (COHP) analysis on selected atomic pairs in the pH range of 7−14. The obtained COHP is integrated up to the Fermi level to yield negative integrated COHP (−ICOHP$_{E_F}$), which acts as a descriptor of the strength of covalent or noncovalent interactions (Figure 5a). It was observed that the Pt−O bond gradually weakens as the pH increases from 7 to 11, sharply reduces to 0.02 eV at pH = 11,

https://doi.org/10.1021/jacs.3c12934
J. Am. Chem. Soc. XXXX, XXX, XXX−XXX

and stays nearly constant thereafter. The Pt−H bond, however, is strengthened from 0 to 0.08 eV after the orientational change from O-down to the position of the atom in water, suggesting a stronger interaction between H in water and the Pt surface at higher pH.

Moreover, the O−H bond in interfacial water is significantly weakened by ca. 0.50 eV in terms of $-ICOHP_{E_F}$ upon the orientational change (Figure 5b). The change in effective pK_a of H-down water is estimated, by the fitted correlation between experimental pK_a and calculated $-ICOHP_{E_F}$ (Figure S9), to be 8 units lower than the neutral O-down case, which agrees reasonably well with acidic-like kinetics suggested in previous experimental reports.[34,35] In addition, the H-down water could act as a relay for protons in the outer water layers to cascade to the Pt surface via a hydronium-like intermediate, which is also in line with recent reports of the higher local concentration of hydronium species near the Pt surface in high-pH conditions.[24] Therefore, more facile Volmer kinetics is expected beyond pH 11 due to the orientational change, which results in the switch of the Tafel slope to a smaller value (Figure 2b).

The molecular origin of the O−H weakening is further analyzed by Bader charge analysis (Figure 5b) and molecular fragment analysis (Figure S10). The net charge of water is ca. + 0.10 |e| in the O-down configuration and −0.06 |e| in the H-down configurations. The partial charging of interfacial water at higher pH can be attributed to the charge redistribution caused by a shift of the work function of the surface. Due to the nonbonding nature of the highest occupied molecular orbital (HOMO; O 2p lone pair), partial removal of an electron from it has little influence on the O−H bond strength. On the other hand, the lowest unoccupied molecular orbital (LUMO) in water has O···H σ^* characteristics (Figure 5b inset), and the filling of this orbital would directly lead to a weakening of the O···H bond, as evidenced by a decrease in Mayer bond order from 0.9 to 0.24 per electron. The diffuse nature of the H-side lobe of the HOMO also promotes the interaction between H in water and the Pt surface.

To quantify the influence of interfacial water configuration on the kinetics of water dissociation, we performed free energy calculations by slow-growth-constrained MD sampling and thermodynamic integration within the FP-AIMD scheme (see Supporting Note 1 for details). Our calculations show that the water with an O-down pH needs to be rotated to a flat configuration before it can break the O···H bond and transfer the H to the Pt surface, with a rather high free energy barrier of 1.10 eV (Figure 5c). In contrast, the H-down water at high pH does not need to go through this extra step and can directly dissociate with a much lower free energy barrier of 0.55 eV. In other words, the interfacial polarization and reorientation of interfacial water molecules to the H-down configuration at high pH not only electronically weakens the O−H in water but also modifies the water dissociation reaction pathway by skipping an intermediate flat configuration, thus greatly reducing the kinetic barrier and leading to considerably improved HER activity.

Additionally, we note that near-surface hydroxide may also play a role in modifying the reaction kinetics, although for technical reasons, it is infeasible to explicitly include solvated hydroxide in the FP-AIMD. To explore this effect, we can derive the difference in thermodynamics of hydroxide binding on the surface from the trajectory averages with and without *OH, assuming the initial state of hydroxide (solvated in the bulk electrolyte) to be pH-independent so that we can cancel out the energy of the solvated state. In this case, our calculations reveal that the hydroxide binding with Pt at higher pH (where the majority of interfacial water is H-down) is stronger than that at lower pH (where the majority of interfacial water is O-down) by 0.25 eV. This indicates the role of interfacial water orientation in stabilizing more surface hydroxide (via water deprotonation or other means) at higher pH values. Such surface hydroxide could also function as electronically favored proton acceptors and geometrically favored proton donors for interfacial H-down water to promote water dissociation.[29]

CONCLUSIONS

In summary, we have performed surface-sensitive electrical transport spectroscopy measurements as well as static and dynamic fixed-potential DFT calculations to understand the molecular-level origin of the pH-dependent HER activity on the Pt surface in alkaline media. The intriguing switching behavior in the pH dependence of interfacial conductance and Tafel slope at ca. pH = 10 suggests a reorganization of the interfacial water molecule structure and a change in the HER mechanism. Static and dynamic calculations reveal a sharp orientation transition of interfacial water from the O-down to H-down configuration, which, as further shown by chemical bonding analysis, leads to a weakened O−H bond and enhanced HER kinetics. Our theoretical results show that the hydroxide binding with Pt at high pH (where the majority of interfacial water is H-down) is stronger than the case at low pH (where the majority of interfacial water is O-down) by 0.25 eV. Such surface hydroxide could function as electronically favored proton acceptors and geometrically favored proton donors for interfacial H-down water to promote water dissociation. The excellent correlation between the experiment and theory provides, for the first time, a robust interpretation of the pH-dependent HER kinetics on the Pt surface in alkaline media. These studies provide a pathway toward a more complete understanding of pH effects on the electrode−water interfacial structure and their critical role in the relevant electrochemical reactions and renewable energy conversion.

ASSOCIATED CONTENT

Supporting Information

The Supporting Information is available free of charge at https://pubs.acs.org/doi/10.1021/jacs.3c12934.

Experimental details; details of the free energy calculation based on fixed-potential MD (Note 1); limitations and justifications of our fixed-potential MD simulations (Note 2); structural characterization of the PtNWs; activation and cleaning of the ETS device; average of normalized conductance from three devices; molecular fragment analysis of charged H_2O; and additional simulations with multiple factors considered (Figures S1−S12) (PDF)

AUTHOR INFORMATION

Corresponding Authors

Anastassia N. Alexandrova − *Department of Chemistry and Biochemistry, University of California, Los Angeles, California 90095, United States; California NanoSystems Institute, University of California, Los Angeles, California*

https://doi.org/10.1021/jacs.3c12934
J. Am. Chem. Soc. XXXX, XXX, XXX−XXX

90095, United States; orcid.org/0000-0002-3003-1911; Email: ana@chem.ucla.edu

Yu Huang − *Department of Materials Science and Engineering and California NanoSystems Institute, University of California, Los Angeles, California 90095, United States;* orcid.org/0000-0003-1793-0741; Email: yhuang@seas.ucla.edu

Xiangfeng Duan − *Department of Chemistry and Biochemistry, University of California, Los Angeles, California 90095, United States; California NanoSystems Institute, University of California, Los Angeles, California 90095, United States;* orcid.org/0000-0002-4321-6288; Email: xduan@chem.ucla.edu

Authors

Aamir Hassan Shah − *Department of Chemistry and Biochemistry, University of California, Los Angeles, California 90095, United States;* orcid.org/0000-0002-0471-4575

Zisheng Zhang − *Department of Chemistry and Biochemistry, University of California, Los Angeles, California 90095, United States;* orcid.org/0000-0002-4370-4038

Chengzhang Wan − *Department of Chemistry and Biochemistry, University of California, Los Angeles, California 90095, United States; Department of Materials Science and Engineering, University of California, Los Angeles, California 90095, United States*

Sibo Wang − *Department of Chemistry and Biochemistry, University of California, Los Angeles, California 90095, United States*

Ao Zhang − *Department of Materials Science and Engineering, University of California, Los Angeles, California 90095, United States*

Laiyuan Wang − *Department of Chemistry and Biochemistry, University of California, Los Angeles, California 90095, United States*

Complete contact information is available at: https://pubs.acs.org/10.1021/jacs.3c12934

Author Contributions

‖A.H.S. and Z.Z. contributed equally to this work.

Notes

The authors declare no competing financial interest.

■ ACKNOWLEDGMENTS

X.D. acknowledges support from the National Science Foundation award 1800580. Y.H. acknowledges support from the Office of Naval Research by grant number N000141812155. Theoretical research was supported by the DOE-BES DE-SC0019152 grant to A.N.A. An award of computer time was provided by NERSC and the Innovative and Novel Computational Impact on Theory and Experiment (INCITE) program. This research used resources from the Argonne Leadership Computing Facility, which is a DOE Office of Science User Facility supported under Contract DE-AC02-06CH11357.

■ REFERENCES

(1) Sheng, W.; Zhuang, Z.; Gao, M.; Zheng, J.; Chen, J. G.; Yan, Y. Correlating hydrogen oxidation and evolution activity on platinum at different pH with measured hydrogen binding energy. *Nat. Commun.* **2015**, *6* (1), No. 5848.

(2) Nørskov, J. K.; Bligaard, T.; Logadottir, A.; Kitchin, J.; Chen, J. G.; Pandelov, S.; Stimming, U. Trends in the exchange current for hydrogen evolution. *J. Electrochem. Soc.* **2005**, *152* (3), J23−J26.

(3) Ledezma-Yanez, I.; Wallace, W. D. Z.; Sebastián-Pascual, P.; Climent, V.; Feliu, J. M.; Koper, M. T. M. Interfacial water reorganization as a pH-dependent descriptor of the hydrogen evolution rate on platinum electrodes. *Nat. Energy* **2017**, *2* (4), 17031−17037.

(4) Bockris, J. O.; Potter, E. The mechanism of the cathodic hydrogen evolution reaction. *J. Electrochem. Soc.* **1952**, *99* (4), 169−186.

(5) Schouten, K. J. P.; van der Niet, M.; Koper, M. Impedance spectroscopy of H and OH adsorption on stepped single-crystal platinum electrodes in alkaline and acidic media. *Phys. Chem. Chem. Phys.* **2010**, *12* (46), 15217−15224.

(6) Strmcnik, D.; Uchimura, M.; Wang, C.; Subbaraman, R.; Danilovic, N.; Van Der Vliet, D.; Paulikas, A. P.; Stamenkovic, V. R.; Markovic, N. M. Improving the hydrogen oxidation reaction rate by promotion of hydroxyl adsorption. *Nat. Chem.* **2013**, *5* (4), 300−306.

(7) Zhong, G.; Cheng, T.; Shah, A. H.; Wan, C.; Huang, Z.; Wang, S.; Leng, T.; Huang, Y.; Goddard, W. A.; Duan, X. Determining the hydronium pKα at platinum surfaces and the effect on pH-dependent hydrogen evolution reaction kinetics. *Proc. Natl. Acad. Sci. U.S.A.* **2022**, *119* (39), No. e2208187119, DOI: 10.1073/pnas.2208187119.

(8) Govindarajan, N.; Xu, A.; Chan, K. How pH affects electrochemical processes. *Science* **2022**, *375* (6579), 379−380.

(9) Greeley, J.; Jaramillo, T. F.; Bonde, J.; Chorkendorff, I.; Nørskov, J. K. Computational high-throughput screening of electrocatalytic materials for hydrogen evolution. *Nat. Mater.* **2006**, *5* (11), 909−913.

(10) Laursen, A. B.; Varela, A. S.; Dionigi, F.; Fanchiu, H.; Miller, C.; Trinhammer, O. L.; Rossmeisl, J.; Dahl, S. Electrochemical hydrogen evolution: Sabatier's principle and the volcano plot. *J. Chem. Educ.* **2012**, *89* (12), 1595−1599.

(11) Skúlason, E.; Tripkovic, V.; Björketun, M. E.; Gudmundsdóttir, S.; Karlberg, G.; Rossmeisl, J.; Bligaard, T.; Jónsson, H.; Nørskov, J. K. Modeling the electrochemical hydrogen oxidation and evolution reactions on the basis of density functional theory calculations. *J. Phys. Chem. C* **2010**, *114* (42), 18182−18197.

(12) Zhu, S.; Qin, X.; Yao, Y.; Shao, M. pH-Dependent Hydrogen and Water Binding Energies on Platinum Surfaces as Directly Probed through Surface-Enhanced Infrared Absorption Spectroscopy. *J. Am. Chem. Soc.* **2020**, *142* (19), 8748−8754.

(13) Sheng, W.; Gasteiger, H. A.; Shao-Horn, Y. Hydrogen oxidation and evolution reaction kinetics on platinum: acid vs alkaline electrolytes. *J. Electrochem. Soc.* **2010**, *157* (11), B1529−B1536.

(14) Subbaraman, R.; Tripkovic, D.; Chang, K.-C.; Strmcnik, D.; Paulikas, A. P.; Hirunsit, P.; Chan, M.; Greeley, J.; Stamenkovic, V.; Markovic, N. M. Trends in activity for the water electrolyser reactions on 3d M (Ni, Co, Fe, Mn) hydr (oxy) oxide catalysts. *Nat. Mater.* **2012**, *11* (6), 550−557.

(15) Durst, J.; Siebel, A.; Simon, C.; Hasché, F.; Herranz, J.; Gasteiger, H. A. New insights into the electrochemical hydrogen oxidation and evolution reaction mechanism. *Energy Environ. Sci.* **2014**, *7* (7), 2255−2260.

(16) van der Niet, M. J. T. C.; Garcia-Araez, N.; Hernández, J.; Feliu, J. M.; Koper, M. T. M. Water dissociation on well-defined platinum surfaces: The electrochemical perspective. *Catal. Today* **2013**, *202*, 105−113.

(17) Goyal, A.; Koper, M. T. M. The Interrelated Effect of Cations and Electrolyte pH on the Hydrogen Evolution Reaction on Gold Electrodes in Alkaline Media. *Angew. Chem., Int. Ed.* **2021**, *60* (24), 13452−13462.

(18) Shen, L.-f.; Lu, B.-a.; Li, Y.-y.; Liu, J.; Huang-fu, Z.-c.; Peng, H.; Ye, J.-y.; Qu, X.-m.; Zhang, J.-m.; Li, G.; Cai, W.-b.; Jiang, Y.-x.; Sun, S.-g. Interfacial Structure of Water as a New Descriptor of the Hydrogen Evolution Reaction. *Angew. Chem., Int. Ed.* **2020**, *59* (50), 22397−22402.

(19) Cheng, T.; Wang, L.; Merinov, B. V.; Goddard, W. A., III Explanation of Dramatic pH-Dependence of Hydrogen Binding on

Noble Metal Electrode: Greatly Weakened Water Adsorption at High pH. *J. Am. Chem. Soc.* **2018**, *140* (25), 7787−7790.
(20) Chen, M.; Zheng, L.; Santra, B.; Ko, H.-Y.; DiStasio, R. A., Jr; Klein, M. L.; Car, R.; Wu, X. Hydroxide diffuses slower than hydronium in water because its solvated structure inhibits correlated proton transfer. *Nat. Chem.* **2018**, *10* (4), 413−419.
(21) Koper, M. T. M. A basic solution. *Nat. Chem.* **2013**, *5* (4), 255−256.
(22) Li, P.; Jiang, Y.; Hu, Y.; Men, Y.; Liu, Y.; Cai, W.; Chen, S. Hydrogen bond network connectivity in the electric double layer dominates the kinetic pH effect in hydrogen electrocatalysis on Pt. *Nat. Catal.* **2022**, *5* (10), 900−911.
(23) Lamoureux, P. S.; Singh, A. R.; Chan, K. pH Effects on Hydrogen Evolution and Oxidation over Pt(111): Insights from First-Principles. *ACS Catal.* **2019**, *9* (7), 6194−6201.
(24) Wang, X.; Xu, C.; Jaroniec, M.; Zheng, Y.; Qiao, S.-Z. Anomalous hydrogen evolution behavior in high-pH environment induced by locally generated hydronium ions. *Nat. Commun.* **2019**, *10* (1), No. 4876.
(25) Jung, O.; Jackson, M. N.; Bisbey, R. P.; Kogan, N. E.; Surendranath, Y. Innocent buffers reveal the intrinsic pH- and coverage-dependent kinetics of the hydrogen evolution reaction on noble metals. *Joule* **2022**, *6* (2), 476−493.
(26) Sun, K.; Wu, X.; Zhuang, Z.; Liu, L.; Fang, J.; Zeng, L.; Ma, J.; Liu, S.; Li, J.; Dai, R.; Tan, X.; Yu, K.; Liu, D.; Cheong, W.-C.; Huang, A.; Liu, Y.; Pan, Y.; Xiao, H.; Chen, C. Interfacial water engineering boosts neutral water reduction. *Nat. Commun.* **2022**, *13* (1), No. 6260.
(27) Ding, M.; He, Q.; Wang, G.; Cheng, H.-C.; Huang, Y.; Duan, X. An on-chip electrical transport spectroscopy approach for in situ monitoring electrochemical interfaces. *Nat. Commun.* **2015**, *6* (1), No. 7867.
(28) Ding, M.; Zhong, G.; Zhao, Z.; Huang, Z.; Li, M.; Shiu, H.-Y.; Liu, Y.; Shakir, I.; Huang, Y.; Duan, X. On-chip in situ monitoring of competitive interfacial anionic chemisorption as a descriptor for oxygen reduction kinetics. *ACS Cent. Sci.* **2018**, *4* (5), 590−599.
(29) Shah, A. H.; Zhang, Z.; Huang, Z.; Wang, S.; Zhong, G.; Wan, C.; Alexandrova, A. N.; Huang, Y.; Duan, X. The role of alkali metal cations and platinum-surface hydroxyl in the alkaline hydrogen evolution reaction. *Nat. Catal.* **2022**, *5* (10), 923−933.
(30) Giles, S. A.; Wilson, J. C.; Nash, J.; Xu, B.; Vlachos, D. G.; Yan, Y. Recent advances in understanding the pH dependence of the hydrogen oxidation and evolution reactions. *J. Catal.* **2018**, *367*, 328−331.
(31) Li, C.-Y.; Le, J.-B.; Wang, Y.-H.; Chen, S.; Yang, Z.-L.; Li, J.-F.; Cheng, J.; Tian, Z.-Q. In situ probing electrified interfacial water structures at atomically flat surfaces. *Nat. Mater.* **2019**, *18* (7), 697−701.
(32) Duan, Z.; Henkelman, G. Atomic-Scale Mechanisms of Electrochemical Pt Dissolution. *ACS Catal.* **2021**, *11* (23), 14439−14447.
(33) Chen, J.-W.; Zhang, Z.; Yan, H.-M.; Xia, G.-J.; Cao, H.; Wang, Y.-G. Pseudo-adsorption and long-range redox coupling during oxygen reduction reaction on single atom electrocatalyst. *Nat. Commun.* **2022**, *13* (1), No. 1734.
(34) Martínez-Hincapié, R.; Sebastián-Pascual, P.; Climent, V.; Feliu, J. M. Exploring the interfacial neutral pH region of Pt(111) electrodes. *Electrochem. Commun.* **2015**, *58*, 62−64.
(35) Rizo, R.; Sitta, E.; Herrero, E.; Climent, V.; Feliu, J. M. Towards the understanding of the interfacial pH scale at Pt(111) electrodes. *Electrochim. Acta* **2015**, *162*, 138−145.

https://doi.org/10.1021/jacs.3c12934
J. Am. Chem. Soc. XXXX, XXX, XXX−XXX